Online ISSN 1848-3380, Print ISSN 0005-1144
ATKAFF 55(1), 22–31(2014)

Aranzazu D. Martin, Jesus R. Vazquez

Backstepping Controller Design to Track Maximum Power in Photovoltaic Systems

DOI 10.7305/automatika.2014.01.289
UDK 681.511.4-531.9:621.314.1; 621.311.243
IFAC 2.3.2; 3.1

Original scientific paper

This work presents a new control method to track the maximum power point of a grid-connected photovoltaic (PV) system. A backstepping controller is designed to be applied to a buck-boost DC-DC converter in order to achieve an optimal PV array output voltage. This nonlinear control is based on Lyapunov functions assuring the local stability of the system. Control reference voltages are initially estimated by a regression plane, avoiding local maximum and adjusted with a modified perturb and observe method (P&O). Thus, the maximum power extraction of the generating system is guaranteed. Finally, a DC-AC converter is controlled to supply AC current in the point of common coupling (PCC) of the electrical network. The performance of the developed system has been analyzed by means a simulation platform in Matlab/Simulink helped by SymPowerSystem Blockset. Results testify the validity of the designed control method.

Key words: Backstepping, Buck-boost converter, Maximum power point (MPP), Photovoltaic system

Sinteza backstepping regulatora za praćenje maksimalne proizvodnje energije u fotonaponskim sustavima. Ovaj rad predstavlja novu metodu upravljanja za slijeđenje točke maksimalne snage fotonaponskog (PV) sustava. Dana je sinteza backstepping regulatora za primjenu u silazno-uzlaznom DC-DC pretvaraču za postizanje optimalnog izlaznog napona PV-a. Ova je nelinearna metoda upravljanja zasnovana na Ljapunovim funkcijama osiguravajući tako lokalnu stabilnost sustava. Upravljačke reference napona prvo su estimirane korištenjem regresijske ravnine izbjegavajući lokalne maksimume, a zatim podešene tzv. modificiranom perturbiraj i uoči metodom (P&O). Prema tome, zagarantirano je maksimalno izvlačenje energije iz sustava proizvodnje. Naposlijetku, DC-AC pretvaračem upravlja se na način da osigurava željena izmjenična struja u točki zajedničkog spoja (PCC) elektroenergetske mreže. Ponašanje razvijenog sustava analizirano je kroz simulacije provedene u Matlab/Simulink okruženju uz korištenje SymPowerSystem biblioteke.

Ključne riječi: Backstepping, silazno-uzlazni pretvarač, točka maksimalne proizvodnje energije (MPP), fotonaponski sustav

1 INTRODUCTION

Nowadays, renewable energy sources are widely used and, particularly, photovoltaic (PV) energy systems have become widespread everywhere. The grid-connected PV systems consist of an array of solar modules, a DC-DC power converter, a DC-AC power converter and a control system. The complete scheme is presented in Fig. 1.

The PV modules convert the solar energy to electrical energy so as to be transferred to the electrical power system [1-2]. The generated power depends on the environment conditions, such as temperature and solar irradiation. Therefore, there is only one operating point with a Maximum Power Point (MPP) under particular conditions by each PV module.

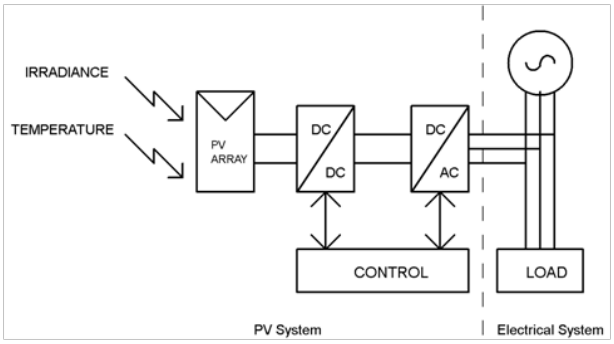

Fig. 1. Structure of the grid-connected PV system

A DC-DC power converter, in this case a buck-boost [3], which converts the DC power from one voltage level to another higher or lower to the input voltage, has to be added at the output of the photovoltaic array to achieve the optimum voltage and to implement the Maximum Power Point Tracking (MPPT).

The MPP can be tracked through different MPPT algorithms that control the switching converter in order to obtain the maximum power under all conditions [4-15]. There are various methods, some of them are based on the well-known principle of perturb and observe (P&O) [7-8], on sliding mode control method [9-10], Ripple Correlation Control (RCC) [11], artificial neuronal networks or fuzzy based algorithms [12-14], amongst others.

In the first method mentioned above, P&O, the output power gets the equilibrium point but it has an oscillatory behavior and that point is not always achieved, obtaining a local maximum instead of a global maximum. The artificial neuronal network has a better performance but presents an involved structure, whereas fuzzy logic control does not need a mathematical model. The methods have different accuracy and complexity.

A new control method for MPPT is proposed in this paper. A nonlinear backstepping controller [16-18] in a buck-boost converter has been designed to track the maximum power point with the help of a regression plane, which provides the PV array output reference voltage helped by a modified P&O method to achieve the MPP faster [19-20]. This case, the duty ratio of the switching converter of the buck-boost converter is controlled. This way, the robustness is increased, global asymptotic stability is guaranteed by means of Lyapunov and the MPP can be assured even with changeable conditions. A nonlinear control has been chosen due to the nonlinear, time variant nature and variable structure of the buck-boost, thus a linear control implies a model linearization that is simple but it cannot control the converter in a wide range.

In addition, the control of the DC-AC power inverter of the PV system has been designed to inject electrical power to the electrical network by means of a PI control [21-22]. So, the global control makes possible extract the maximum power of the PV system, inject active power and regulate the input voltage of the DC-AC power inverter.

The paper is organized as follows. Section 2 presents the PV system model, describing the model of the PV array and the buck-boost converter. The proposed design of the control to make the system track the maximum power point is developed in Section 3, where the regression plane and the backstepping controller are explained, this section also includes the design of the control of the inverter. Section 4 presents the simulation results and Section 5 describes the main conclusions.

2 PV SYSTEM MODEL

The model of the photovoltaic system is shown in this section. Firstly, it will be presented the model of the solar cell, secondly, the DC-DC power converter modeling and, finally, the inverter model.

2.1 Model of the PV array

The solar cell turns the light into electrical energy. Its well-known model consists of a current source I_l that represents the current generated by the photons, (it will be constant if the radiation and the temperature are constants too), in A, an anti-parallel diode D_1, a shunt electrical resistance R_{sh}, in Ω, which represents the current leakage, and a series resistance R_s, in Ω, which models the ohmic losses. The equivalent circuit is shown in Fig. 2.

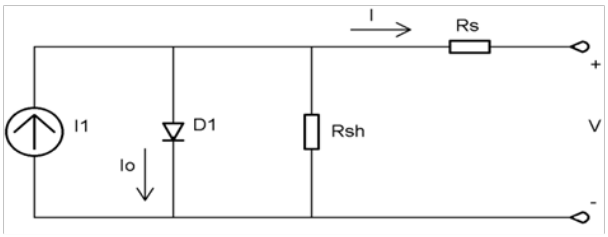

Fig. 2. Equivalent circuit of a PV cell

The equation that relates I, the solar cell output current in A, to V, the solar cell output voltage, in V, is shown in (1):

$$I = I_l - I_o \left(e^{q\frac{(V+R_s I)}{nKT_K}} - 1 \right) - \frac{V + R_s I}{R_{sh}}, \qquad (1)$$

where I_l is the light generated current, in A, I_o is the cell reverse saturation current, in A, q is the charge of an electron, in C, n is the ideal factor (dimensionless), K is the Boltzmann's constant, in J/K and T_K is the working temperature of the cell, in K [10].

Therefore, the solar cells are connected in series and in parallel in order to create a solar module depending on the capacity demands. The array used in this work has been modeled in a real installation and it has sixteen modules that consist of 72 solar cells in series and one solar cell in parallel. There are four modules shunt connected and four modules in parallel. The voltage will be obtained multiplying the voltage of one solar cell by the number of cells connected in series whereas the current will be calculated multiplying the current of a solar cell by the number of cells that are shunt connected.

Under standard conditions, 1000 $\mathrm{W/m^2}$ and 25 °C, the electrical parameters of the solar system are shown in Table 1.

Table 1. Electrical parameters of the solar module

Parameter	***Values***
Maximum power	1555 W
Maximum power voltage	102.6 V
Maximum power current	15.16 A
Open-circuit voltage	165.8 V
Short-circuit current	17.56 A

There is only one operating point for a PV array with a maximum output power that changes with the cell temperature, T in °C, and the solar radiation, G in $\mathrm{W/m^2}$. The MPPs with different irradiations and a cell temperature of 25 °C are presented in Table 2.

Table 2. Maximum power points to 25 °C and changeable irradiance

Radiation (W/m²)	***Maximum Power (W)***
200	383
400	748
600	1066
800	1332
1000	1555
1200	1733

If the irradiance and temperature of the whole PV array is homogeneous, the power curve of the system has an only maximum. In partial shading conditions, the P-V curve has several local maximum but one global maximum point [23]. In sections 3.1 and 3.2, the proposed control will be detailed in order to prove that the global maximum is achieved helped by a plane regression that places the system close to the maximum point.

2.2 Model of the buck-boost converter

Figure 3 shows the topology of the buck-boost power converter used in this work. It consists of power electronic components such as capacitor and inductor elements connected as is shown in the Fig. 3. In closed loop, the function of the control is to regulate the voltage of the solar modules, in order to achieve the maximum power, by means of the control of the duty cycle, D.

The ON/OFF commutation of the switch, controlled by means of Pulse Width Modulation (PWM) principle, allows the charge and discharge of energy of the storage elements, getting an output voltage higher or lower to the input voltage. The transistor T_1 and the diode D_2 imply a non-linear behavior of the converter.

The output voltage of the DC-DC power converter is v_o in V, v_{PV} is the input voltage of the converter or the output voltage of the solar array in V, i_{PV} is the output current of the PV array, in A, and i_L is the inductor current in A. In

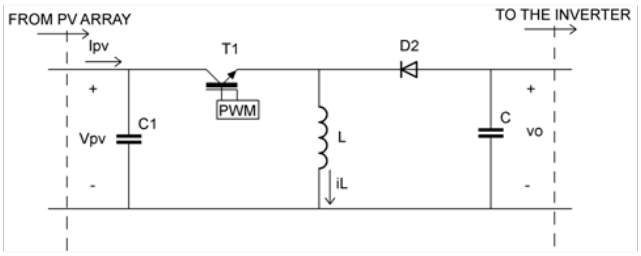

Fig. 3. Buck-boost power converter

this case, the load is a resistance. Parameters R, L, C_1 and C (resistance in Ω, inductor in H and capacitors in F) are constants.

The duty cycle of the converter is $D = t_{ON}/t_C$, being t_{ON} the time which the switch is ON and t_C is the switching period ($0 < D < 1$).

When the switch is ON, the PV array supplies energy to the inductor and the diode is inversely polarized and the charge is insulated from the source. Thus, the supplied energy is stored in the inductor. When the switch is OFF, the diode conducts and the stored energy in the inductor is transferred to the charge.

The converter can work in two modes, Continuous Conduction Mode (CCM) and Discontinuous Conduction Mode (DCM), depending on the current of the inductor in the operation period. In CCM, the current of the inductor is never zero, the current fluctuates between maximum and minimum values based on the time that the switch is ON. In DCM, when the switch is OFF there is a time which the current of the inductor is zero because t_{OFF}, the time which the switch is OFF, is greater than the time that the inductor can transfer energy. Thus, the inductor is completely discharged.

In this work, the DC-DC converter will work in CCM. In order to guarantee this mode, the minimum value of the inductor and the capacitor must be calculated as is shown in (2) and (3) [25]:

$$L_{\min} = \frac{(1 - D_{\min})^2 v_o}{2 I_{o\,\min} f_s}, \tag{2}$$

$$C_{\min} = \frac{I_{o\,\max} D_{\max}}{\Delta v_o f_s}, \tag{3}$$

where Δv_o is the incremental output voltage of the buck-boost converter, $D_{\min}$ and $D_{\max}$ are the minimum and maximum duty cycle respectively, $I_{o\,\min}$ and $I_{o\,\max}$ are the minimum and maximum output current of the DC-DC converter and f_s is the frequency.

Thus, the system ranges from short-circuit voltage to open-circuit voltage in order to obtain the I-V character-

istics of the solar modules. The buck-boost converter provides an output impedance that changes from zero to infinite.

The output voltage of the buck-boost converter has opposite polarity from the input voltage. Besides, the output/input ratio can be determined as it is shown in (4):

$$\frac{v_o}{v_{PV}} = \frac{D}{1-D}. \tag{4}$$

Using the state averaging method [24], the model can be defined as are shown in (5), (6) and (7):

$$\dot{v}_{PV} = \frac{1}{\mathrm{C}_1} i_{PV} - \frac{1}{\mathrm{C}_1} i_L D, \tag{5}$$

$$\dot{i}_L = \frac{v_o}{\mathrm{L}} + \frac{v_{PV} - v_o}{\mathrm{L}} D, \tag{6}$$

$$\dot{v}_o = -\frac{i_L}{\mathrm{C}} - \frac{v_o}{\mathrm{RC}} + \frac{i_L}{\mathrm{C}} D. \tag{7}$$

Duty cycle must be controlled so as to get the voltage with which it is obtained the maximum energy.

2.3 Model of the inverter

The DC-AC power inverter connects the PV system to the electrical network. Its aim is to provide the maximum active power to the network.

A three-phase inverter has been used in this work. It consists of a control circuit to calculate the reference current and a power circuit to follow this reference and to inject the final current to the network. The power circuit includes six insulated-gate bipolar transistors (IGBT) devices with anti-parallel diodes to get the desired AC output with a specific sequence of commutation of the transistors. Two capacitors have been included in order to regulate the voltage. The DC-AC topology is shown in Fig. 4. The output of the DC-DC power converter will be connected with the DC side.

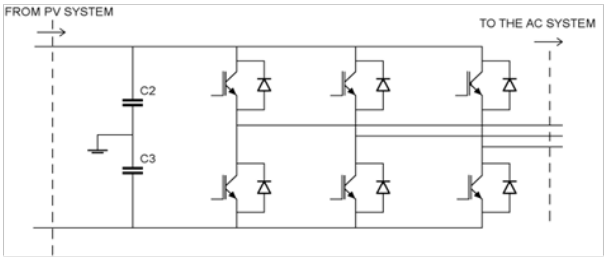

Fig. 4. DC-AC power converter

The DC-AC outputs are connected to the network through output reactance to establish a pulse-width modulation (PWM) current control. In this work, a hysteresis-band technique has been used [26].

3 CONTROL DESIGN

The main objective of the proposed control is to adjust the PV array output reference voltage, given by a regression plane, using a backstepping controller to regulate the DC-DC input voltage and to guarantee the maximum energy extraction of the PV modules. Thereby, the local maximum is avoided adjusting the reference voltage instead of the duty cycle in P&O method.

Then, the optimum voltage must be obtained modifying the voltage around the reference or theoretical voltage according to a backstepping controller instead of a standard PI control. This control is required to achieve the voltage that supplies the maximum power at the input of the converter.

A control strategy for the inverter has been proposed to supply active power to the electrical system.

3.1 Maximum power reference voltage

A regression plane gives the reference or theoretical voltage to achieve the MPP under any conditions of temperature and solar radiation. This way, the MPPT block reaches the value of the voltage that supplies the maximum power, and the peak of the power curve is achieved initially faster. Even if there are several local maximum (for example, a partial shading case), the proposed control approaches initially to the global maximum and it does not stay at a local maximum.

Firstly, the characteristic curves of the system are obtained. Secondly, the regression plane is calculated for a variety of cell temperatures and solar radiation. The regression plane is shown in Fig. 5.

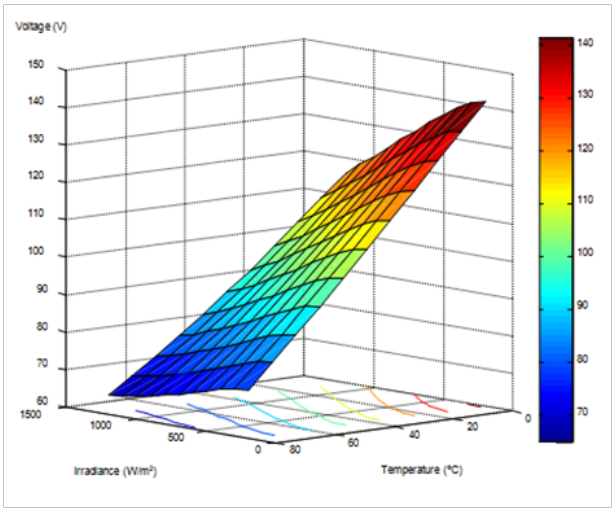

Fig. 5. MPP Reference voltage depending on irradiance and temperature

Temperature T ranges from 0 °C to 80 °C whereas the irradiance ranges from 200 $\mathrm{W/m^2}$ to 1000 $\mathrm{W/m^2}$. A voltage matrix is obtained for the maximum power depending on the environmental conditions. Thus, the reference voltage is calculated by linear interpolation and the backstepping controller will take into account the reference voltage supplies by the plane regression.

3.2 Buck-boost backstepping controller

The aim of this control is to extract the maximum power. In order to do this, a non-linear backstepping controller is designed to control the duty cycle of the switch of the buck-boost converter. This way, the output voltage of the PV modules can be regulated to track the reference voltage.

The backstepping control is used to design stable controls with a recursive methodology. It must stabilize the origin of a system by means of feedback control laws and using Lyapunov functions to prove the stability of the system.

In this case, next steps should be followed to design the controller.

Firstly, the voltage error is defined as is shown in (8):

$$e_{_1} = v_{PV} - v_{PV}^r, \tag{8}$$

where v_{PV}^r is the reference output voltage of the PV modules and it must be reached by the control in order to enforce v_{PV} to its appropriate value. Deriving e_1 with respect to time and accounting for (5), (9) is obtained:

$$\dot{e}_{_1} = \dot{v}_{PV} - \dot{v}_{PV}^r = \frac{1}{C_1} i_{PV} - \frac{1}{C_1} i_L D - \dot{v}_{PV}^r. \tag{9}$$

In (9), i_L behaves as a virtual control input. Now, a Lyapunov function is selected. It must be positive definite and radially unbounded for all x, and the time derivative of Lyapunov function must be negative definite for all x to assure the solution is locally asymptotically stable. The chosen function and its derivative are defined as:

$$V_{_1} = \frac{1}{2} e_1^2, \tag{10}$$

$$\dot{V}_{_1} = e_1 \dot{e}_1 = e_1 \left(\frac{1}{C_1} i_{PV} - \frac{1}{C_1} i_L D - \dot{v}_{PV}^r \right) = -k_1 e_1. \tag{11}$$

$\dot{V}_{_1}$ will be negative if k_1 is constant and positive. This way, the reference current for the control, α_1, so-called stabilization function, can be obtained working out the value of the i_L from (11):

$$\alpha_{_1} = (C_1 k_1 e_1 + i_{PV} - C_1 \dot{v}_{PV}^r) \frac{1}{D}. \tag{12}$$

Next step must study the behavior of the current error, $z_1 = i_L - \alpha_1$, where the inductor current should reach α_1 to make the error vanish in order to achieve the control aim. The time derivative of this error is shown in (13):

$$\dot{z}_1 = \dot{i}_L - \dot{\alpha}_1. \tag{13}$$

Now, the time derivative of α_1, (12), replacing i_L by $z_1 + \alpha_1$, yields (14):

$$\dot{\alpha}_1 = k_1 z_1 - \frac{C_1 k_1^2}{D} e_1 - \frac{C_1}{D} \ddot{v}_{PV}^r + \frac{1}{D} \dot{i}_{PV} - \alpha_1 \frac{\dot{D}}{D}. \tag{14}$$

Equation (14) with (6) gives the time derivative of z_1, as is shown in (15):

$$\dot{z}_1 = \frac{v_o}{L} + \frac{v_{PV} - v_o}{L} D - \left(k_1 z_1 - \frac{C_1 k_1^2}{D} e_1 - \frac{C_1}{D} \ddot{v}_{PV}^r + \frac{1}{D} \dot{i}_{PV} - \alpha_1 \frac{\dot{D}}{D} \right). \tag{15}$$

Similarly to which it is done in the Lyapunov function V_1, another Lyapunov function should be defined with the same characteristics, being as (16):

$$V_2 = V_1 + \frac{1}{2} z_1^2 = \frac{1}{2} e_1^2 + \frac{1}{2} z_1^2. \tag{16}$$

And its time derivative is (17), accounting for (9) and (15), and replacing i_L by $z_1 + \alpha_1$:

$$\dot{V}_2 = -k_1 e_1^2 + z_1 \left[\frac{v_o}{L} + \frac{v_{PV} - v_o}{L} D + e_1 \left(\frac{C_1 k_1^2}{D} - \frac{D}{C_1} \right) - k_1 z_1 + \frac{C_1}{D} \ddot{v}_{PV}^r - \frac{1}{D} \dot{i}_{PV} + \alpha_1 \frac{\dot{D}}{D} \right] = -k_1 e_1^2 - k_2 z_1^2. \tag{17}$$

Equation (17) will be negative when k_2 is positive, being a constant, in order to ensure the stability of the system. Therefore, the term between square brackets must be zero, thus working out the value of the controller $\dot{D}$, yields (18):

$$\dot{D} = \frac{1}{\alpha_1} \Big[- \frac{v_o}{L} D - \frac{v_{PV} - v_o}{L} D^2 - e_1 \left(C_1 k_1^2 - \frac{D^2}{C_1} \right) + z_1 (k_1 - k_2) D - C_1 \ddot{v}_{PV}^r + \dot{i}_{PV} \Big], \tag{18}$$

where $0 < D < 1$ and $\alpha_1 \neq 0$.

In order to prove that the controller is locally asymptotically stable in the equilibrium point, a study of the stability will be carried out.

Firstly, the errors should be defined taking into account the references, as follows in (19), the error of the voltage,

(20), the error of the current and, (21), the error of the controller:

$$e_1 = v_{PV} - v_{PV}^r, \tag{19}$$

$$e_2 = i_L - i_L^r, \tag{20}$$

$$e_3 = D - D^r. \tag{21}$$

This way, the time derivatives of the errors are (22), (23) and (24), replacing v_{PV}, i_L and D by $e_1+v_{PV}^r$, $e_2+i_L^r$ and $e_3 + D^r$ respectively, and using (5) and (6):

$$\dot{e}_1 = \frac{1}{C_1} i_{PV} - \frac{1}{C_1}(e_2 + i_L^r)(e_3 + D^r), \tag{22}$$

$$\dot{e}_2 = \frac{v_o}{L} + \frac{e_1 + v_{PV}^r - v_o}{L}(e_3 + D^r), \tag{23}$$

$$\begin{aligned}\dot{e}_3 = \frac{1}{\alpha_1}\Big[&- \frac{v_o}{L}(e_3 + D^r) - \\ &\frac{e_1 + v_{PV}^r - v_o}{L}(e_3 + D^r)^2 - \\ &e_1\left(C_1 k_1^2 - \frac{(e_3 + D^r)^2}{C_1}\right) + \\ &z_1(k_1 - k_2)(e_3 + D^r) - C_1 \ddot{v}_{PV}^r + \dot{i}_{PV}\Big].\end{aligned} \tag{24}$$

It must be known that the last two terms are zero because v_{PV}^r and i_{PV} are constants. To obtain locally asymptotically stability, the errors and its derivatives will be zero in the equilibrium point. Thus, the references values can be calculated as in (25), (26) and (27):

$$v_{PV}^r = \frac{-v_o + v_o D^r}{D^r}, \tag{25}$$

$$i_L^r = \frac{i_{PV}}{D^r}, \tag{26}$$

$$D^r = \frac{v_o}{v_o - v_{PV}^r}. \tag{27}$$

In (27), $v_0 < 0$ and $v_{PV}^r > 0$, thus $0 < D^r < 1$. Next step is to get the Jacobian in the equilibrium point, where the errors are zero and v_{PV}^r is the reference voltage at the input of the DC-DC converter, so as to achieve the eigenvalues to ensure the locally stability. Hence, the obtained reference values assure that the real part of the Jacobian eigenvalues is negative, thus the locally asymptotically stability is guaranteed.

In Section 4, a numerical example will be presented to check the proposed control.

Figure 6 shows the DC-DC converter control scheme. On the one hand, with the regression plane and T and G values, the theoretical reference voltage is obtained. On the other hand, taking into account i_{PV} and v_{PV}, a modified P&O method is applied. This proposed method is based on the traditional P&O, but it provides an incremental value of reference voltage instead of the duty cycle value. The addition of theoretical reference voltage and the incremental reference voltage gives the final reference voltage used in backstepping control. In order to implement this method, it is necessary to take into account $v_{ref,f}$, i_{PV}, v_{PV}, v_o and i_L. Hence, equation (18) is implemented so as to get the duty cycle that controls the DC-DC converter.

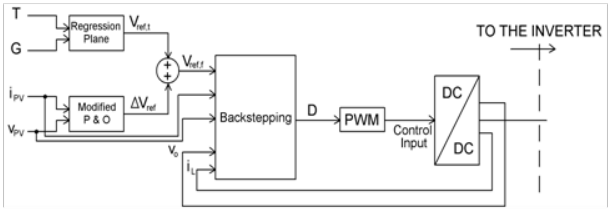

Fig. 6. Control scheme of the DC-DC converter

3.3 Inverter control strategy

The designed control strategy supplies electrical power to the electrical system. This method has been proposed because it is effective, simple and easy to implement with a reduced computation time.

The PV power system injects AC current to the electrical network, i_{AC} in A. In this work, the aim of the inverter control is to inject current co-linear with the voltage in point of common coupling. Thus, the current reference is shown in (28):

$$i_{AC,ref} = K\, v_{AC}, \tag{28}$$

where K is an adjustment parameter and it can be adjusted by a PI control, Fig. 7. and v_{AC} is the PCC alternating voltage. If the error between $i_{AC,ref}$ and the inverter output current, i_{AC} is bigger than a hysteresis band [26], the state of the appropriate semiconductors will change to follow the reference. The frequency of the switching depends on current changes from the upper to lower limit or vice versa. Equation (28) assures the power grid synchronization because the output current of the system and the voltage of the common connection point are in phase with each other.

Note that the reference voltage at the input inverter is set at 600 V, greater than the grid voltage so as to guarantee correct working of the inverter [27]. Hence, the aim of the control is to keep constant this voltage. This way, on the one hand, if the voltage of the PV system is greater than reference voltage, the energy of the solar modules is stored in the capacitor and it is not injected to the AC system. On the other hand, if the voltage of the PV system is lower than 600 V, the load requires more power than the PV system can supply, thus the source must supply the rest of the active power that it is necessary.

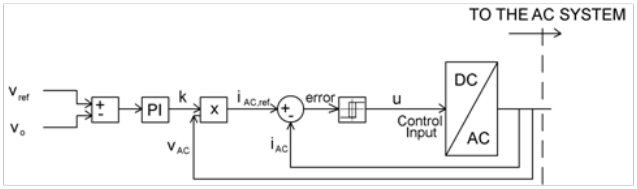

Fig. 7. Control scheme of the DC-AC converter

The inverter control strategy is shown in Fig. 7. The v_{ref} is 600 V, v_o is the output voltage of the DC-DC converter and u is the signal control of the inverter.

4 RESULTS

A practical case has been simulated in Matlab/Simulink, using SimPowerSystem blockset, to validate the proposed control. The PV system is connected to a radial electrical network with a three-phase source and a resistive load, Fig. 8. The PV array block models sixteen PV modules according to Fig. 6. The DC/DC block, the DC/AC block (without capacitors), the backstepping control block and the inverter control block were shown in figures 3, 4, 6 and 7 respectively.

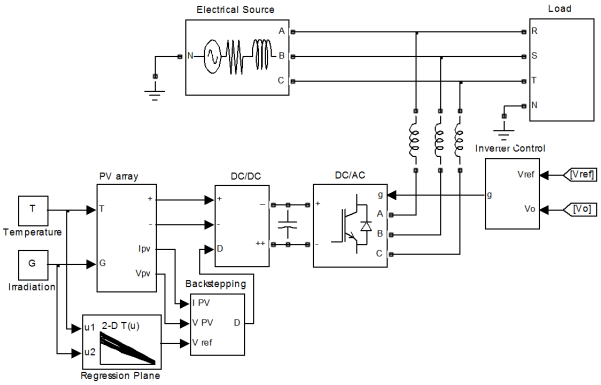

Fig. 8. Simulink block diagram of the system

The simulation parameters and other element values are presented in Table 3.

Table 3. Simulation parameters

Parameter	***Values***
k_1	60
k_2	9000
L	20e-3 H
C	48e-6 F
C_1	1e-3 F
R	50 Ω

k_1 and k_2 are the parameters used in backstepping method, in (18), L is the inductor of the DC-DC converter, C_1 and C are the capacitor at the input of the buck-boost converter and the capacitor of the DC-DC converter respectively whereas R is the load resistor at the AC side.

The system has been simulated for changeable environmental conditions. Thus, a change of the solar radiation of the whole system from 600 $\mathrm{W/m^2}$ to 1000 $\mathrm{W/m^2}$ at 0.3 s was considered, as it is shown in Fig. 9.a, with a temperature of 25 °C, to prove that the MPP is always achieved and to check the transient performance of the designed controller. This way, the robustness of the system with changes of solar radiation is evaluated.

In Fig. 9.b and Fig. 9.c, the voltage and the power are presented with their references values respectively where it is shown the controller tracking behavior. The reference voltage is reached by the voltage that supplies the PV array, whereas the maximum power is achieved as well.

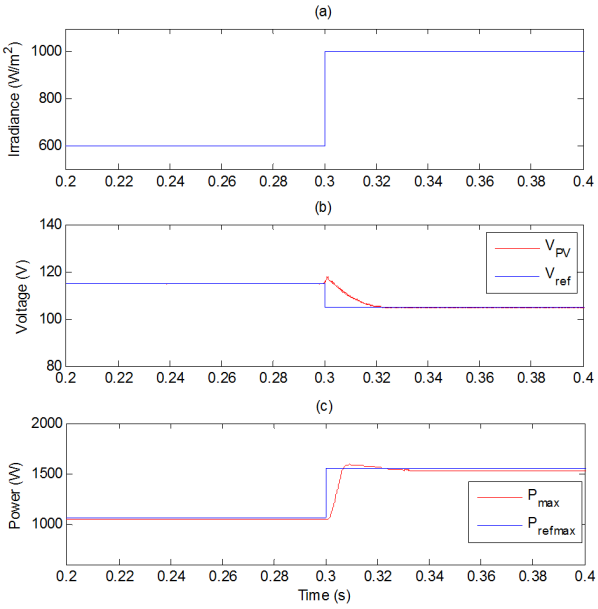

Fig. 9. Results of backstepping controller (a) irradiance, (b) DC voltage, (c) PV power

According to the Table 2, the maximum power is 1066 W when the irradiance is 600 $\mathrm{W/m^2}$ and the temperature is 25 °C, and the maximum power for 1000 $\mathrm{W/m^2}$ and 25 °C is 1555 W. The reached powers are 1047 W and 1531 W respectively, instead of the maximum power due to the losses in the buck-boost converter. However, there are only slight losses and the performance of the system is 98.46%, quite satisfactory. Besides, the transient response of the system is satisfactory, because it is stabilized after a smooth transient response in less than two periods. This way, the validation of the system using backstepping con-

troller is guaranteed and the maximum power point is always achieved with low losses.

Moreover, as it is shown in Fig. 10.a, the inverter control detailed in Fig. 7 allows to obtain a constant voltage at the input of the DC/AC converter even though there are changeable environmental conditions; in the studied case, the maximum variation of voltage is 0.5% in transient period, from 0.3 s to 0.317 s. Besides, figures 10.b and 10.c show the voltage and the current at the output of the inverter. The alternating voltage at the output of the DC/AC inverter, Fig. 10.b, is stable without transient perturbances whereas the current at the output of the inverter, Fig. 10.c, depends on the supplied power of the PV system.

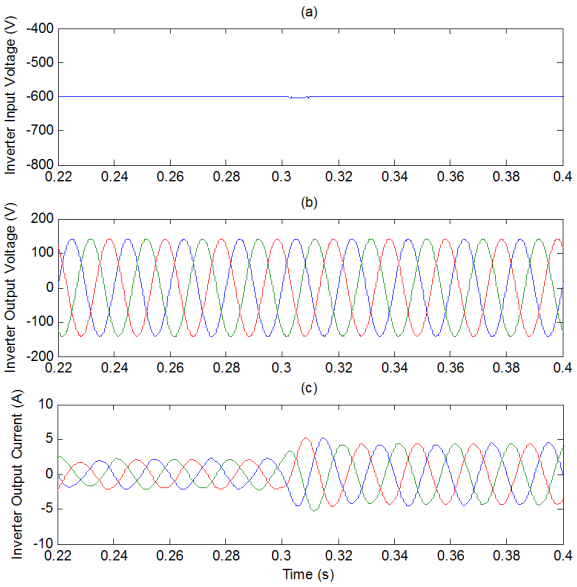

Fig. 10. Simulation results of the inverter control. (a) inverter input DC voltage, (b) inverter output AC voltage, v_{AC}, (c) inverter output AC current, i_{AC}

In the previous case, a homogeneous irradiance of the whole system has been considered. Thus, the PV curve shows an only peak. The proposed control allows to achieve the global maximum power point even if there are more than a peak. A partial shading case has been simulated in order to prove the correct working of the proposed controller when there are several peaks in the P-V curves.

This case, there are two shaded modules in series and the rest of the modules are not shaded. The irradiance and temperature in shaded modules are 500 $\mathrm{W/m^2}$ and 25 °C respectively whereas the environmental conditions in not shaded modules are 1000 $\mathrm{W/m^2}$ and 25 °C. In these conditions, the P-V curve has two maximums, but the global maximum is 1302 W with 110 V, Fig. 11.

Therefore, the power at the output of the DC-DC converter is close to the global maximum, as it is shown in Fig. 12.

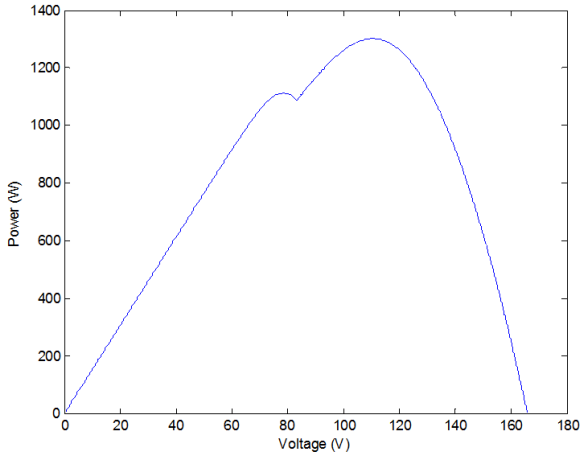

Fig. 11. P-V curve with multiple maximum

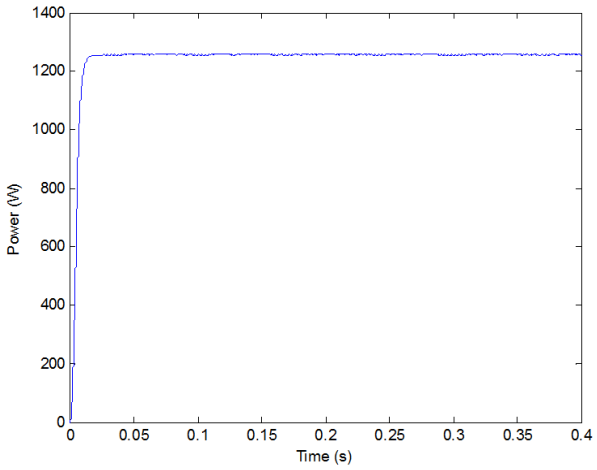

Fig. 12. Output power with multiple maximum

The maximum achieved is 1256 W and the local maximum is avoided.

5 CONCLUSION

In this work, a novel backstepping controller to track the MPP of a PV system has been designed. This nonlinear controller has been applied to a buck-boost converter to achieve the PV array output voltage which obtains the maximum power for all environmental conditions, checking the robustness for different values of solar radiation. The control reference voltage has been obtained with the help of a regression plane. Furthermore, the global asymptotic stability of the controller has been proved.

The simulation results show the performance of the PV system is 98.46% and the transient response is about 0.04 s with sudden changes in environmental conditions.

The output power has been injected to an AC electrical system through a DC/AC converter. The control of this inverter has been validated in the simulation platform. The inverter input voltage remains constant and the output voltage is stationary for all conditions of the system. The injected currents depend on the available output power. Besides, the proposed method has been validated with two peaks power curve to check that the local maximum is avoided.

To sum up, it has been proved the usefulness and the effectiveness of the backstepping method to control a buck-boost converter to extract the maximum power of a PV system, contrasting the results in a numerical simulation.

A possible extension of this work could be to improve the control of the DC-AC power inverter in order to add new functions to the PV system, such as electrical system conditioning. The inverter could inject reactive power and harmonic current to compensate the non-linear loads of the electrical system. This way, the Power Quality (PQ) of the electrical network would be improved.

Next research step will be to develop an experimental platform where the whole system could be proved. This paper has been made with this final objective, for this the PV array model is a grid-connected real system available by the authors in the research group installation.

ACKNOWLEDGMENT

This work was supported by the MEC (Ministerio de Educación of Spain) under FPU grant (Formación de Profesorado Universitario).

The authors are with the Electrical Engineering Department at Escuela Técnica Superior de Ingeniería in University of Huelva, Spain (e-mail: aranzazu.delgado@die.uhu.es; vazquez@uhu.es).

REFERENCES

[1] M. Buresch, “Photovoltaic Energy Systems Design and Installation”, McGraw-Hill, New York, 1983.

[2] I. H. Altas1 and A.M. Sharaf, “A Photovoltaic Array Simulation Model for Matlab-Simulink GUI Environment”, *IEEE International Conference on Clean Electrical Power,* ICCEP ’07, pp. 341-345.

[3] Tasi-Fu Wu; Yu-Kai Chen, “Modeling PWM DC/DC Converters out of Basic Converter Units”, *IEEE Transactions on Power Electronics*, vol. 13, no. 5, pp. 870-881, 1998.

[4] A. Daoud, A. Midoun, “Simulation and Experimental Study of Maximum Power Point Tracker Based on a DC/DC Buck Converter”, *International Review of Electrical Engineering,* vo. 5. No. 2, Part A, pp. 514-520, April 2010.

[5] Tirshan Esram and Patrick L. Chapman, “Comparison of photovoltaic array maximum power point tracking techniques”, *IEEE Transactions on Energy Conversion*, vol. 22, no. 2, June 2007.

[6] Doron Shmilovitz, Yoash Levron, “Distributed Maximum Power Point Tracking in Photovoltaic Systems – Emerging Architectures and Control Methods”, *Automatika*, vol. 53, no. 2, pp. 142-155, 2012.

[7] Villalva, M.G.; Gazoli, J.R.; Filho, E.R., “Analysis and simulation of the P&O MPPT algorithm using a linearized PV array model”, *Power Electronics Conference, 2009. COBEP ’09. Brazilian*, pp. 189-195, 2009.

[8] Elgendy, M. A.; Zahawi, B.; Atkinson, D. J., “Evaluation of Perturbe and Observe MPPT Algorithm Implementation Techniques”, *6th IET International Conference on Power Electronics, Machines and Drives (PEMD 2012)*, pp. 1-6, 2012.

[9] Miao, Z., W. Jie, et al., “The application of slide technology in PV maximum power point tracking system”, *Fifth World Congress on Intelligent Control and Automation*, WCICA, 2004.

[10] M. I. Arteaga Orozco, J. R. Vázquez, P. Salmerón, “MPP Tracker of a PV System using Sliding Mode Control with Minimum Transient Response”, *International Review on Modelling and Simulations (I.RE.MO.S.)*, December 2010.

[11] T. Esram, J.W. Kimball, P.T. Krein, P.L. Chapman, P. Midya, “Dynamic maximum power point tracking of photovoltaic arrays using ripple correlation control”, *IEEE Transactions on Power Electronics,* vol. 21, No. 5, pp. 1282-1291, September 2006.

[12] Ramaprabha, R.; Mathur, B.L.; Sharanya, M., “Solar Array Modeling and Simulation of MPPT using Neural Network”, *International Conference on Control, Automation, Communication and Energy Conservation*, pp. 1-5, 2009.

[13] Syafaruddin, Karatepe, E., Hiyama, T., “Artificial neural network-polar coordinated fuzzy controller based maximum power point tracking control under partially shaded conditions”, *IET Renewable Power Generation*, vol. 3, no. 2, pp. 239-253, June 2009.

[14] Theodoros L. Kottas, Yiannis S. Boutalis and Athanassios D. Karlis, “New Maximum Power Point Tracker for PV Arrays Using Fuzzy Controller in Close Cooperation With Fuzzy Cognitive Networks”, *IEEE Transactions on Energy Conversion,* vol. 21, no. 3, September 2006

[15] Giovanni Petrone, Giovanni Spagnuolo, Massimo Vitelli, “Distributed Maximum Power Point Tracking: Challenges and Commercial Solutions”, *Automatika*, vol. 53, no. 2, pp. 128-141, 2012.

[16] Youping Zhang, Barıs¸ Fidan, Petros A. Ioannou, “Backstepping Control of Linear Time-Varying Systems with Known and Unknown Parameters”, *IEEE Transactions on Automatic Control*, vol. 48, no. 11, November 2003.

[17] El Fadil, H.; Girt, F., “Backstepping Based Control of PWM DC-DC Boost Power COnverters”, *Symposium on Industrial Electronics, ISIE 2007*, pp. 395-400, 2007.

[18] Fan Liping; Yu Yazhou; Boshnakov, K., "Adaptative Backstepping Based Terminal Sliding Mode Control for DC-DC Convertor", *International Conference on Computer Application and System Modeling (ICCASM 2010)*, pp. V9-323-V9-327, 2010.

[19] Michael Sokolov and Doron Shmilovitz, "A Modified MPPT Scheme for Accelerated Convergence", *IEEE Trans. On Energy Conversion*, vol. 23, no. 4, December 2008, pp. 1105-1107.

[20] Sachin Jain and Vivek Agarwal, "A New Algorithm for Rapid Tracking of Approximate Maximum Power Point in Photovoltaic Systems", *IEEE Power Electronics Letters*, vol. 2, no. 1, March 2004, pp. 16-19.

[21] Minaei, S.; Yuce, E.; Tokat, S.; Cicekoglu, O., "Simple Realizations of Current-Mode and Voltage-Mode PID, PI and PD Controllers", *Proceedings of the IEEE Internationsl Symposium on Industrial Electronics, ISIE*, vol. 1, pp. 195-198, 2005.

[22] Georgios Tsengenes, Georgios Adamidis, "Comparative Evaluation of Fuzzy-PI and PI Control Methods for a Three Phase Grid Connected Inverter", *Proceedings of the 2011-14th European Conference on Power Electronics and Applications (EPE 2011),* 2011.

[23] Paraskevadaki, E.V.; Papathanassiou, S.A., "Evaluation of MPP Voltage and Power of mc-Si PV Modules in Partial Shading Conditions", *IEEE Transactions on Energy Conversion*, vol. 26, no. 3, pp. 923-932, 2011.

[24] R. Ortega, A. Lorai, P. J. Niklasson and H. Sira-Ramirez, "Passivity-based Control of Euler-Lagrange Systems", London: Springer-Verlag, pp. 168-171, 1998.

[25] Rashid Muhammad H., "DC DC Convertes" in *Power Electronics Handbook*, Ed. Academic Press, 2001, pp. 216-224.

[26] Devaraj, D.; Sakthivel, S.; Punitha, K., "Modeling of Photovoltaic Array and Simulation of Adaptive Hysteresis Current Controlled Inverter for Solar Application", *3rd International Conference on Electronics Computer Technology (ICECT)*, vol. 6, pp. 302-306, 2011.

[27] P. Salmerón, J.; J. R.Vázquez; "Active Power Line Conditioners" in A. Moreno, *Power Quality, Mitigation Technologies in a Distributed Environment*, Ed. Springer, London, 2007, pp. 231-291 19.

Aránzazu D. Martín was born in Bollullos del Condado, Huelva, Spain, on December 21, 1983. She received the degree in Industrial Engineering from the University of Huelva, Spain, in 2008. She did a master in Control Engineering, Electronic Systems and Industrial Computer Science in 2011. Since 2008, she has been collaborating with the Electrical Engineering Department at University of Huelva. She is currently working as a researcher with the FPU grant. Now, her research interests include renewable energy, distributed electrical generation, power quality, active power filter and fuzzy logic.

Jesús R. Vázquez was born in Huelva, Spain, on December 24, 1967. He received the degree in electrical engineering from the University of Seville, Spain, in 1995. He obtained the Ph.D. degree in 2004. For one year, he was with the electrical department of Nissan Motor Ibérica S.A., Barcelona, Spain. Since 1996, he is with the Electrical Engineering Department at the Escuela Técnica Superior de Ingeniería of the University of Huelva. He teaches Electric Circuits, Electrical Power Quality and Photovoltaic Systems and his research interests include power quality, active power filters, renewable energy, distributed electrical generation and artificial network applications.

AUTHORS' ADDRESSES

Aránzazu D. Martín, M.Sc.
Prof. Jesús R. Vázquez, Ph.D.
Electrical Engineering Department,
Escuela Técnica Superior de Ingeniería,
University of Huelva,
Ctra. Palos de la Frontera s/n, Palos de la Frontera,
ES-21819, Huelva, Spain
email: aranzazu.delgado@die.uhu.es, vazquez@uhu.es

Received: 2012-06-04
Accepted: 2012-10-24